Synthesis and Characterization of Versatile Polymer Particles for the Adsorption of Bromophenol Blue and Phenol

Kutalmis Gokkus (kgokkus@kastamonu.edu.tr)
Kastamonu University
Cigdem Oter
Van Yuzuncu Yil University
Merilyn Amlani
Mindanao State university, Tawi-Tawi College of Technology and Oceanography
Mahmut Gur
Kastamonu University
Vural Butun
Osmangazi University

Research Article

Keywords: Polymeric particles, adsorption, bromophenol blue, phenol

Posted Date: October 28th, 2023

DOI: https://doi.org/10.21203/rs.3.rs-3481924/v1

Additional Declarations: No competing interests reported.

Abstract

Removing anionic pollutants from water sources remains a major challenge in supramolecular chemistry. Today, cellulose, activated carbon, zeolite, and similar materials, which are widely preferred, have a weak effect against anionic pollutants. Therefore, further modifications are needed for the use of such substances. On the contrary, in this study, highly functional and economical polymeric particles (called GD particles) were synthesized with high yield and did not require further modifications. GD particles were synthesized with glutaraldehyde and diethylenetriamine as monomers for the first time. The structural properties of the synthesized particles were characterized by FT-IR, TGA, and SEM analyses. Then, GD particles were used in the adsorption of anionic Bromophenol blue and phenol. The isotherm, thermodynamic, and kinetic models were used to explain the adsorption mechanism between Bromophenol blue, phenol, and GD particles. Thus, it was determined that the adsorption process between GD particles and Bromophenol blue was chemisorption, and between phenol and GD particles, physical adsorption took place. It was determined that GD particles polymer particles had high adsorption capacities, such as 136.40 mg/g for bromophenol blue and 98.26 mg/g for phenol than natural adsorbents. As a result, it was produced economical, simple, feasible, and functional adsorbents against anionic pollutants.

1. Introduction

Adsorption of anionic pollutants in water remains a significant challenge in synthetic supramolecular chemistry (Gale et al., 2018; Ong et al., 2020). Because to retain an anionic pollutant in water, adsorbents must meet the energy requirement for the desolvation of the anions (Cremer et al., 2018; Sullivan et al., 2018). Polar, electrostatic interactions and/or combinations can meet this energy. For example, positively charged adsorbents can interact electrostatically with anions. Likewise, Lewis acids can form coordinated bonds with anions in water. On the other hand, polar groups (-OH, -NH, etc.), hydrophobic groups (-CH, aromatic structure, etc.), and neutral structures containing halogens or π-bonds interact with anions.

Within the scope of this study, two different models of anionic pollutants (Bromophenol blue, BPB, and phenol, PH) belonging to two different pollutant types (dyes and organic pollutants) were selected. Because the dye industry and its wastes were considered one of the most important sources of pollutants that caused water pollution (Altaher et al., 2014; Ghaedi et al., 2014; Ahmed and Abou-Gamra, 2016; Xiang et al., 2019). In addition, most of the dyes used in the industry are anionic dyes, and they contain disease-causing and carcinogenic groups (Bhaumik et al., 2013; Nayunigari et al., 2017; You et al., 2018; Guo et al., 2019; Feng et al., 2020; Xu et al., 2020). In addition, they can change water resources' physical and chemical properties even at very low concentrations. Most importantly, dyes are used extensively in almost every industry. In other words, tons of dye are produced and used yearly (Yagub et al., 2014). This means that large quantities of dye are wasted in water sources. On the other hand, PHs, which are organic pollutants, especially those containing chlorine, are considered priority pollutants (Aygun et al., 2003). Phenols are environmentally important aromatic organic compounds and have attracted much

attention recently due to their high toxicity to human and living health (Alves et al., 2020; Demissie et al., 2021). It is one of the primary pollutants in most chemical and petrochemical industries, such as coal refineries, paper, plastics, and agriculture. Therefore, pollutants such as dye and PH must be effectively treated and/or taken under control, especially to protect water resources.

Today, activated carbon (AC), cellulose, starch, glucose, zeolite, and similar substances frequently remove pollutants because they are natural, cheap, and abundant. These substances contain a large number of oxygen-containing functional groups. The strong electronegative nature of the oxygen atom make them polar. Thanks to this polarity, such substances are highly effective against cationic pollutants, while their effect is weak against anionic contaminants. For instance, Altaher et al. (2014) produced ACs from date pits and used these ACs in the adsorption of Eriochrome Black T and BPB. As a result, these ACs' adsorption capacity was found 36.5 and 39.68 mg/g, respectively. In another study, ACs were produced from banyan root for PH adsorption (Nirmala et al., 2021). Although the surface areas of these ACs were very high (988 m^2/g), their PH removal capacity was relatively low (26.95 mg/g). Therefore, such substances must be modified for high efficiency anion removal. For example, the surface of cellulose was modified with 2,3-epoxypropyl trimethyl ammonium chloride (EPTMAC) (Kono et al., 2016; Feng et al., 2020). After this modification, the surface of the cellulose gained a cationic character. The adsorption capacity of this modified cellulose for Eosin Y dye increased to 364.22 mg/g (Feng et al., 2020). While Mhlongo et al. (2022) modified the surface of the cellulose with glycidyl-trimethylammonium chloride, Liu et al. (2022) used ethylenediamine. Alorabi et al. (2020) produced natural composite materials from Fe_3O_4, CuO, and AC to enhance the AC adsorption performance against BPB. The adsorption capacity of these composites was 88.60 mg/g for BFB. In the other study, natural sepiolite was treated only with acid (Pardo et al., 2018). After acid treatment, the adsorption capacity of this natural sepiolite was determined 37 mg/g for methylene blue (MB). Lütke et al. (2019) produced ACs from black wattle bark with $ZnCl_2$ for PH adsorption. They reported that the capacities of these ACs were 98.57 mg/g.

On the other hand, when studies on the adsorption of anionic pollutants were examined, it was understood that amine and imine groups had high affinities towards anionic pollutants. Because amine and imine groups changed the surface charge of the adsorbents. For example, β-cyclodextrin contains many -OH groups in its structure. As a result of the modification of these groups with ethanolamine, 602 and 1085 mg/g yields were obtained against methyl orange (MO) and Congo red (CR) anionic dyes, respectively (Jiang et al., 2020). After modification, zeta measurements showed the surface of the β-cyclodextrin gained cationic properties due to the presence of amine and imine groups. Feng et al. (2020) revealed that polyethyleneimine-grafted celluloses adsorbed approximately 83 times more anionic dyes than original cellulose. In the same study, cationic cellulose foams were also synthesized. These foams showed 364.22 and 193.8 mg/g adsorption performance against Eosin Y and Malachite green dyes, respectively. Similarly, Song et al. (2016) synthesized amine-containing biopolymer resins for the adsorption of anionic dyes MO, Reactive Brilliant Red K-2BP (RBR), and Acid Red 18 (AR). The adsorption capacities of these resins were calculated as 101.0 mg/g, 222.2 mg/g, and 99.4 mg/g, respectively. In another study, it was determined that the capacities of glucose beads functionalized with amines were

1487.29 mg/g and 699.30 mg/g for MO and tartrazine (TTZ) dyes respectively (Liu et al., 2022). Therefore, it was understood that the presence of amine and/or imine groups was very significant for the removal of an anionic pollutants.

In this study, polymer particles that are both cheap like natural materials and have high amine and imine contents were produced with glutaraldehyde (GA) and diethylenetriamine (DETA). Glutaraldehyde is a highly reactive dialdehyde that reacts easily and quickly with nucleophiles such as amines, hydroxyls, and thiols under mild conditions. Due to these advantages, it was used in scientific studies for many years (Genta et al., 1998; Ramires and Milella, 2002; Migneault et al., 2004; Kulkarni et al., 2007; Bolto et al., 2009; More et al., 2010; Martinez et al., 2014; Li et al., 2018; Anrades et al., 2019; Gao et al., 2022; Khan et al., 2022; Abellanas-Perez et al., 2023). Diethylenetriamine, on the other hand, contains three amine groups in its structure and therefore has high reactivity. Thus, it was used in materials science for many years in many different disciplines, from polymers to metals and biomaterials (Senkal and Bicak, 2001; Kasgoz et al., 2003; Zahng et al., 2009; Wang et al., 2013; Lavrenyuk et al. 2016; Yang et al. 2020; Hasan et al., 2021; Mohd et al. 2021; Jiang et al., 2022; Zelenka et al. 2022; Gao et al., 2023; Gokkus et al. 2023). In short, it is understood that both molecules will be used in many scientific studies in the future, as in the past, due to their high reactivity, cheap and high reaction efficiency. However, interestingly, in our literature research, we could not find the synthesis of polymer particles with GA and DETA. Therefore, GA and DETA used as monomers for the first time to obtain highly functional polymeric particles (called GD particles) in this study.

An adsorbent should be economical and highly effective against the target pollutant. One of the reasons why scientists concentrated their studies on cellulose, AC, zeolite, and similar materials was that these materials were economical. From this point of view, it was aimed to synthesize simple, feasible, and applicable (for many fields) polymeric particles with high amine and imine content that did not require any modification in this study. This was achieved by polymerizing glutaraldehyde (GA) and diethylenetriamine (DETA) as monomers for the first time. Afterward, these polymeric particles were successfully used in the adsorption of anionic BFB and PH (Fig. 1).

2. Materials and Methods

2.1. Synthesis of GD polymer particles

After adding 80 mL (0.212 mol, 1.5 equivalents) of GA to the round bottom reaction flask, the balloon was closed with a septum to provide an inert environment. Meanwhile, 15.25 mL (0.141 mol, 1.0 equivalent) of DETA was added to a separate vial, and the vial was closed with a septum similarly. Both solutions were degassed separately with N2 gas for 20 minutes. Then, a cannula added the DETA solution to the GA solution at room temperature. The solution was stirred at a slow mixing speed until the formation of polymeric particles of tile color (the characteristic color of Schiff bases; Fig. 2). At the end of the reaction, GD particles were washed three times with distilled water (DW), ethanol (EtOH), acetone (AC),

tetrahydrofuran (THF), DW, and AC, respectively. Thus, unreacted GA and DETA were removed. Finally, the particles were dried in a freeze dryer and made ready for characterization and adsorption.

2.2. Characterization of GD polymer particles

SEM images for the morphologies of GD particles were obtained with the FEI Quanta FEG250 device. Chemical characterization was determined by Bruker Alpha model FT-IR instrument. Thermogravimetric analyses (TGA) were carried out with a Tetra SII Exster 6000 device at a rate of 5°C/min in a nitrogen atmosphere between 25°C and 800°C.

2.3. Adsorption studies

All adsorption experiments were carried out in triplicate according to the batch adsorption method. The effects of pH (2, 4, 6, 8 ve 10), temperature (25, 35, 45 ve 50ºC), contact time (0–210 mins), initial dye concentration (40, 80, 100, 250, 300, 400 ve 500 ppm) and GD dose (10, 25, 50, 75 ve 100 mg) on the adsorption capacity of GD particles were completed according to the procedure reported by Shahbazi et al (2011). In all adsorption studies, the solution volume was 25 mL, and the shaking speed of 150 rpm was kept constant. The concentration or absorbance of BPB and PH solutions before and after the adsorption experiments were measured using the Hach Lange DR9000 UV Spectrophotometer at wavelengths 589 and 270 nm, respectively. The adsorption capacity and removal efficiency (%) of GD particles were calculated by Equation (I) and Equation (II), respectively:

$$q_e = \frac{(C_o - C_e)}{W} V \, (\mathbf{I})$$

$$Removal Efficiency \, (\%) = \frac{(C_o - C_e)}{C_o} x100\% \, (\mathbf{II})$$

where V (L) is the solution volume, Co and Ce (mg/L or ppm) represent the initial and final solution concentration of BPB dye, respectively, and W (g) is the adsorbed dry mass.

3. Results and Discussion

3.1. Characterization

The chemical structure of the synthesized polymeric particles was revealed using FT-IR spectroscopy. The FT-IR spectra of all the samples were recorded in transmission mode using a Bruker-Alpha spectrometer ranging the wave number from 4000 to 400 cm-1. The FT-IR spectrum of GD particles was shown in Fig. 3. Aliphatic -CH2-stretching vibrations were observed in relatively broad bands under 3000 cm-1 at 2928 and 2862 cm-1, while the peaks at 1439 and 1358 cm-1 were their bending vibrations. The broad peak at 3350 cm-1 was due to water adsorbed by GD particles, also seen in the TGA. Many peaks observed on this peak could belong to amine groups likely present in the resulting polymer end-groups. The strong peak in 1659 cm-1 was vibrations of imine groups (C = N), which were abundant in the

structure of polymeric particles. On the left side of the imine peak, a peak (1697 cm-1) belonging to the C = C binary group was seen as a shoulder. Additionally, an amine bending peak was observed at 1609 cm-1.

The surface morphologies of GD particles were elucidated by SEM analysis. SEM micrographs obtained at different scales (200 and 500 nm and 2 μm) were given in Fig. 4. It was seen from the images that the polymer particles were successfully synthesized. Particle sizes were determined with the ImageJ software. The diameters of 106 different particles in the 2 μm SEM image were measured for this. Accordingly, it was determined that the average particle size was 703 nm, the smallest particle was 195 nm, and the largest particle was 1146 nm.

Thermal stability and decomposition of GD particles were determined by using TGA analysis. TGA analysis was conducted by heating the sample from room temperature to 800 ºC at a heating rate of 5 oC/min under a nitrogen atmosphere. The thermogram of GD particles was depicted in Figure S1. Accordingly, weight loss was seen in two stages. In the first stage, a weight loss of about 5% (5.26%) occurred in the weight of the polymer particles up to 105 ºC. The mass loss in this first stage was thought to be due to water loss. The second weight-loss stage started at 200 ºC and ended at 500 ºC. A weight loss of approximately 73% (73.11%) occurred at this stage. After the temperature of 200 ºC, the polymer particles started to decompose and completely decomposed at 500 ºC. After this second stage, approximately 22% (21.63%) of the mass remained as char.

3.2. Adsorption experiments

Contact time effect and adsorption kinetics

Adsorption is an equilibrium process involving the interactions between adsorbate and adsorbent. Correctly determining the contact time between the adsorbate and the adsorbent is the first step for the most efficient use of the adsorbent. If this time is insufficient, the adsorption process cannot continue effectively. Otherwise, it will lead to a waste of time and energy. Therefore, this study determined contact times for BPB and PH first. Experiments were conducted between 0–210 min for BPB (300 mg/L BPB concentration, 25ºC, and 50 mg GD particles) and 0–150 min for PH (pH 5.5, 25ºC, 15 mg GD particles, 50 mg/L PH concentration) (Fig. 5). Accordingly, BPB was rapidly adsorbed on GD particles for up to 180 minutes. After this time, this increase in adsorption stopped. Therefore, the adsorption contact time for BPB was determined to be 180 minutes. A similar trend was observed for PH, and PH's contact time was 30 min. Subsequent experiments were carried out over these times.

Adsorption is a time-dependent process, and the equilibrium time is proportional to the adsorption rate. Therefore, the adsorption rate is essential when choosing an effective adsorbent to remove impurities from the solution (Repo et al., 2011). Adsorption kinetics are calculated with this change in adsorption rate depending on time. These calculations determine the possible mechanism of dye adsorption on the adsorbent surface. Therefore, in order to understand the mechanism of adsorption between BPB, PH, and GD particles, the pseudo-first-order (PFO) kinetic model (Lagergren, 1898), pseudo-second-order (PSO)

kinetic model (Ho and McKay, 1999), Weber-Morris intraparticle diffusion (Weber and Morris, 1963) and Elovich (Chien and Clayton, 1980) kinetic models were used. Models and calculations were presented in the “Supplementary document."

The results for the four models were given in Table 1, and the graphs obtained were given in Figures S2 and S3, respectively. The PFO model assumes that the occupancy rate of the adsorption sites is proportional to the number of occupied sites. In contrast, the PSO model considers that the occupancy rate of the adsorption sites is proportional to the square of the number of occupied sites (Altaher et al., 2014). Accordingly, when the correlation coefficients (R2) calculated with the PFO and PSO models for BPB were compared, the R2 of the PSO model was found to be higher (0.98). That was, the adsorption for BPB fits the PSO kinetic model. This fitting showed that the rate-limiting step could be chemisorption involving valence forces through sharing or electron exchange between GD particles and BPB [10]. In addition, the adsorption energy in the Dubinin-Radushkevic (D-R) isotherm revealed that the adsorption had a chemical character. At the same time, when the calculated qe (111.89 mg/g) and experimental qe (94.33 and 99.8 mg/g, respectively) amounts for both models were compared, it was understood that the PSO model was more appropriate

for the adsorption.

Adsorption generally occurs in three mass transfer stages, depending on time. The first is the external diffusion of dye molecules in the liquid phase to the adsorbent surface. The second is the intraparticle diffusion of dye molecules into the pores of the adsorbent, and the third is the formation of physical or chemical bonds of the adsorbate at the active centers in the pores of the adsorbent (Ahmed and Abou-Gamra, 2016). Therefore, the linearity of the graphs obtained by kinetic studies does not cover the entire time interval. On the contrary, they exhibit multicollinearity, revealing the existence of successive adsorption steps. The adsorption process between GD particles and BPB occurred in two stages, as seen in the graph obtained by Weber-Morris intraparticle diffusion (Figure S3c). Accordingly, the adsorption capacity increased rapidly up to 43.36 mg/g in the first stage, and then this increase rate slowed down in the second stage. Since the active sites on the surface of GD particles were empty at the beginning of the adsorption (first step), BPB molecules were rapidly adsorbed to these sites. Therefore, in the first stage, adsorption took place rapidly. In the second step, where the adsorption rate decreased, BPB molecules diffused into the pores of GD particles. Therefore, the rate of adsorption decreased.

The Elovich equation is a kinetic model that explains chemical adsorption on heterogeneous solid surfaces. The correlation coefficient (R2 = 0.98) showed that the fit of this model was the same as for PSO. These results showed that the adsorption between GD particles and BPB fits the PSO and Elovich kinetic model. In other words, it was understood that the surface of GD particles was heterogeneous, and chemical adsorption took place between GD particles and BPB. When the kinetic models for PH adsorption were examined, the correlation coefficient (0.9968) was higher in the PSO kinetic model. At the same time, the calculated qe,cal values (25.32 mg/g) were extremely close to the experimental qe,exp value (25.98 mg/g). Thus, the PSO kinetic model proved to be more suitable to represent the kinetics of

PH adsorption on GD particles (Table 1). As is well known, the PSO model is based on the hypothesis that valence forces can control the rate-limiting step through electron sharing or exchange between adsorbent and adsorbate [31]. This result was also consistent with the kinetic behavior of PH adsorption on other adsorbents (Juang et al., 2000; Mohanty et al., 2005). In summary, the PSO kinetic model, which fitted well with PH adsorption, showed that the adsorption process was due to the interaction between the π-electrons in the PH ring and the basal plane of GD particles (Coughlin and Ezra, 1968).

Table 1
Kinetic parameters of PH and BPB adsorption on GD particles

Models	Parameters	GD particles	
		PH	BPB
Pseudo-first order	q_e ($mg.g^{-1}$)	23.8	111.89
	k_1 (min^{-1})	0.08	-0.016
	R^2	0.9936	0.970
	q_{exp} ($mg.\ g^{-1}$)	25.98	94.33
Pseudo-second order	q_e ($mg.g^{-1}$)	25.32	111.89
	k_2 ($g.mg^{-1}.min^{-1}$)	0.01	0.00036
	R^2	0.9968	0.98
	q_{exp} ($mg.g^{-1}$)	25.98	99.8
Weber-Morris intra-particle diffusion	k_i ($mg.\ g^{-1}min^{-1/2}$)	4.24	3.05
	I ($mg.g^{-1}$)	1.34	10.49
	R^2	0.9694	0.90
Elovich	α ($mg.g^{-1}min^{-1}$)	6.33	5,28
	β ($g.mg^{-1}$)	0.145	0,088
	R^2	0.9929	0,98

Effect of pH

pH changes the surface charge of the dyes and adsorbents and the degree of protonation of the functional groups in the adsorbent. In short, since the change in pH seriously affects the adsorption process, it is necessary to determine the optimum pH. Therefore, experiments were conducted with GD

particles for the adsorption of BPB dye at different pHs (2, 4, 6, 8, and 10) (25ºC, 50 mg GD particles, 100 ppm BPB concentration, and 180 min). Accordingly, the lowest BPB adsorption was determined at pH 2 (27.61 mg/g) and the highest at pH 4 (48.85 mg/g) (Fig. 6a). The adsorption efficiency decreased after this pH. The pKa value of BPB, a weakly acidic dye, was 4.10 (Ghaedi et al., 2014; Liu et al., 2014; Xiang et al., 2019). Therefore, BPB was anionic in an acidic medium. On the other hand, Zeta Potential measurements (25.5 mV and 0.0802 ms/cm) showed that the surface of GD particles was cationic (Figure S4). In addition, GD particles had amino groups in their structure. It was also well known that amino groups become quaternized by protonation in acidic environments and acquire cationic properties. Briefly, the anionic structure of BPB and the gaining cationic properties of GD particles in acidic conditions increased their electrostatic interaction. As a result, the highest adsorption efficiency was achieved at pH 4. The low BPB adsorption at pH 2 could be explained by the medium's highly increased number of protons. The protons surrounded BPB molecules (with electrostatic interactions) and created a steric barrier between GD particles and BPB. In addition, it was known that the adsorption of anionic dyes decreased with increasing pH, and the adsorption of cationic dyes increased (You et al., 2006). On the other hand, to determine the optimum pH for PH adsorption onto GD particles, experiments were performed between pH 4 and 10 (30 min, 25ºC, 15 mg GD, 50 mg/L PH concentration). The amount of adsorbed PH reached its maximum value at pH 5 and tended to decrease at higher and lower pH values (Fig. 6b). This decrease in pH values other than pH 5 may be due to the anionic character of PH and the cationic character of GD particles, as in BPB adsorption. Adsorption of PH molecules was adversely affected due to the suppression of increased proton and hydroxyl groups in the environment (Djebbar et al., 2012).

Initial BPB and PH concentration effects and adsorption isotherms

Determining the optimum dye concentration for an adsorbent is one of the essential parameters to reveal the use potential or capacity. Therefore, with different initial BPB concentrations (40–500 mg/L), the optimal BPB concentration for GD particles was determined (25ºC, 50 mg GD particles, and 180 min; Fig. 7a). The adsorption efficiency of GD particles increased rapidly from 40 mg/L to 300 mg/L concentration (from 19.23 mg/g to 111.90 mg/g), after which the increase did not change much (from 111.90 mg/g to 116.58 mg/g). Up to 300 mg/L concentration, BPB molecules were rapidly adsorbed on the surface of GD particles, after which the adsorption rate decreased markedly. This rapid increase could be explained by the increasing amount of BPB molecules repel each other. Under the influence of this possible repulsion, BPB molecules rapidly diffused to the surface of GD particles. This may have triggered both faster adsorption and better diffusion of particles into the pores of GD particles. As a result, 300 mg/L was determined as the most suitable BPB concentration for GD adsorbent.

Regarding PH, the effect of different initial concentrations (5-250 mg/L) was demonstrated by shaking the PH solution at 15 mg GD particles and pH 5 for 30 minutes (Fig. 7b). Accordingly, the highest PH removal efficiency was 88.9% for the initial 10 mg/L PH concentration. Adsorption sites and specific adsorbent surfaces were more attractive at low PH concentrations, so the removal efficiency was high. In

the opposite case, the removal efficiency decreased due to the saturation of the adsorption areas quickly (Es'haghi et al., 2016).

Experimental data tests in Langmuir (Langmuir, 1916), Freundlich (Freundlich, 1906), Temkin (Temkin and Pyzhev, 1940), and Dubinin-Radushkevich (D-R) (Dubinnin and Radushkevich, 1947) isotherm models were performed for this study to evaluate the adsorption equilibrium process and to comprehensively investigate and reveal the interaction between BPB, PH and GD particles. Details of models and calculations were given in the "Supplementary document."

Parameters of all isotherms for BPB and PH adsorption on GD particles were presented in Table 2, and graphs of isotherms were depicted in Figures S5 and S6, respectively. Isotherm calculations and graphs for BPB were created using data obtained with 300 ppm BPB concentration. Accordingly, the highest R2 value of 0.9998 among all isotherms for BPB was obtained in the Langmuir isotherm. This showed that the adsorption was monolayer and homogeneous. The calculated qm and experimental qe results (120.48 mg/g and 111.89 mg/g, respectively) also supported these results. On the other hand, the adsorption energy (119.02 J/mg) calculated for BPB with the Temkin isotherm clearly revealed that the adsorption process was endothermic. Therefore, there was a strong interaction between BPB and GD particles. It was also explained in the section where the effect of temperature on adsorption was explained that the adsorption process was endothermic (Fig. 9). In order to decide on the adsorption type, the adsorption energy values calculated from the D-R adsorption isotherm were used. The fact that the adsorption energy calculated by the D-R isotherm (E = 691.07 kJ/mol) was greater than 16 kJ/mol indicated a chemical adsorption process between GD particles and BPB.

As in BPB, the highest R2 (0.9941) was determined for PH adsorption in the Langmuir model. This showed that PH molecules were adsorbed on the GD particles' surface in a monolayer and homogeneous manner. The fact that the maximum monolayer adsorption capacity (qm; 107.53 mg/g) calculated from the Langmuir isotherm model was very close to the experimental results (qe; 98.26 mg/g) supported that monolayer adsorption took place. Similarly, Sridar et al. (2018), in their study of PH adsorption on zinc oxide (ZnO) nanoparticles, stated that Langmuir isotherm showed good agreement with PH removal data compared to other isotherms. Another study, which determined the PH adsorption capacity with clay-carbon composites, reported that the Langmuir isotherm was the most suitable isotherm model for adsorption (Tümsek and Demir, 2019). The n values calculated from the Freundlich isotherm equation were 1.66 for PH. Since this value was in the range of $1 < n < 10$, it can be concluded that adsorption was feasible. On the other hand, regarding PH adsorption, the adsorption energy for the D-R isotherm was calculated as 0.75 kJ/mol. The fact that this energy was lower than 8 kJ/mol indicated that the adsorption of PH molecules on GD particles occurred in physical adsorption. Therefore, it could be said that there were weak Van der Waals attraction forces between GD particles and PH molecules. In addition, the differences between the calculated qm and experimental qe results (89.35 mg/g and 111.89 mg/g, respectively) were acceptable, and the correlation coefficient was 0.98, which also supported the chemical nature of adsorption.

Table 2
Isotherm parameters of phenol and BPB adsorption on GD particles

Models	Parameters	GD particles	
		Phenol	BPB
Langmuir	q_{max} ($mg.g^{-1}$)	107.53	120.48
	$q_{e,exp}$ ($mg.g^{-1}$)	98.26	111,89
	K_L ($L.mg^{-1}$)	0.04	0.13
	R_L	0.7	0.16
	R^2	0.9941	0.9998
Freundlich	K_f $[(mg.g^{-1})(L.mg^{-1})^{1/n}]$	6.27	22.45
	n	1.66	2.97
	R^2	0.9811	0.903
Temkin	β_T	19.5	20.43
	KT ($L.g^{-1}$)	0.72	1.93
	R^2	0.9536	0.963
Dubinin-Radushkevich	q_{max} ($mg{\cdot}g^{-1}$)	50.82	89.35
	$q_{e,exp}$ ($mg.g^{-1}$)	98.26	111,89
	β ($mol^{-2}.J^{-2}$)	0.9	$1.04*10^{-6}$
	E ($kJ.mol^{-1}$)	0.75	692.26
	R^2	0.6817	0.979

Adsorbent dosage

Determining the optimum amount of adsorbent for adsorption is very important in terms of not decreasing the adsorption efficiency and increasing the cost. If the amount of adsorbent is kept low, the surface area of the adsorbent and the number of active sites will not be sufficient to adsorb the dye at the desired concentrations. The use of high amount of adsorbent will not be economical. Therefore, experiments were conducted to determine the optimum amount of adsorbent (between 10 and 100 mg)

(25ºC, 100 ppm BPB concentration, and 180 min). Accordingly, the adsorption efficiency of GD particles decreased as the amount of adsorbent increased. The highest adsorption capacity was determined at the amount of 10 mg adsorbent (104.10 mg/g), and the lowest capacity was determined at the amount of 100 mg adsorbent (22.98 mg/g) (Fig. 8a). The agglomeration of GD particles could explain the decrease in adsorption efficiency with the amount of adsorbent during the process (it may be that the agitation speed was insufficient for the amount of adsorbent 100 mg). The possibility of agglomeration of GD particles made it difficult for BPB molecules to diffuse into or onto the adsorbent surface. Therefore, this effect was dominant above the amount of 100 mg adsorbent. Similar results were obtained in highly cross-linked polyamine folic acid (PFCs) polymers synthesized by the polycondensation technique (Nayunigari et al., 2017). In the adsorption of Congo red, it was stated that the active sites were closed due to agglomeration of the polymers, and the adsorption efficiency decreased. In experiments to determine the effect of adsorbent dose on PH adsorption, despite the amount of adsorbent varying in the range of 5-120 mg, the initial PH concentration was 50 mg/L, contact time 30 min, pH 5, temperature adjusted to 25°C (Fig. 8b). Maximum adsorption efficiency (85.2%) was obtained when the adsorbent dose was 15 mg. As the amount of adsorbent increased, the adsorption efficiency decreased.

Effect of Temperature and Chemical Thermodynamics

Experiments were carried out at different temperatures (15–50 ºC) (50 mg GD particles, 100 ppm BPB concentration, and 180 min) to investigate the effect of temperature on the adsorption process. Accordingly, the lowest result (112.231 mg/g) was obtained at 25 ºC and the highest (136.40 mg/g) at 50 ºC. Results increased slightly from 25 ºC to 45 ºC (Fig. 9a). At 50 ºC, the adsorption efficiency reached its maximum level with a sudden increase. This continuous increase indicated that the adsorption process was endothermic. In other words, as the temperature increased, more BPB molecules were adsorbed on the surface of GD particles. In order to determine the effects of temperature on PH adsorption, at temperatures ranging from 20–50 ºC, PH solutions at an initial concentration of 50 mg/L at pH 5.0 were shaken for 30 minutes. As the temperature increased, the adsorption capacity increased, as shown in Fig. 9b. The optimum temperature value was found to be 50 ºC. This showed that the adsorption reaction also occurred endothermically for PH.

Evaluation of the adsorption process from a thermodynamic point of view is critical to deciding whether adsorption is spontaneous. In this study, these evaluations were made using thermodynamic parameters such as Gibbs free energy, enthalpy, and entropy changes. The equations used for the calculations were given in the "Supplementary document."

In order to calculate the adsorption thermodynamic function values such as ΔG°, ΔS° and ΔH°, adsorption experiments were carried out at 25°C, 35°C, 45°C and 50°C with 300 ppm BPB concentration and 50 mg GD particles. The adsorption process usually takes place at constant pressure. Therefore, the thermodynamic function Gibbs free energy change (ΔG°) was used to decide whether the adsorption process was stable at constant pressure. Since the reaction changes with time or the adsorption process takes place, whether the reaction is spontaneous is determined by the decrease or increase of ΔG°

(Aliabadi et al., 2013). When the data in Table 3 were examined, it was determined that the ΔG° value calculated for all temperatures varied between − 0.98 and − 4.33 kJ/mol. The negative Gibbs free energy indicated that adsorption was voluntary and spontaneous. The standard enthalpy change (ΔH°) represented the heat change for reactions under constant pressure. A negative value indicated that the system gave off heat (exothermic), and a positive value indicated that the reaction received heat (endothermic). As a result of the calculations, the ΔH° value was found to be 31.96 kJ/mol. That was, the adsorption between GD particles and BPB was endothermic. This showed why the adsorption efficiency between GD particles and BPB increased with increasing temperature. If the standard entropy change (ΔS°), which indicates the disorder in the reaction, is positive, the randomness increases during adsorption. As a result of the experiments, the ΔS° value of 109.22 J/mol K for GD particles indicated that the adsorption at the GD particles and BPB interface increased irregularity.

Thermodynamic parameters calculated for PH adsorption on GD particles were also given in Table 3. Accordingly, negative ΔG° values, as in BPB, indicated that PH adsorption was a spontaneous and positive process. In addition, the fact that the ΔG° value becomes more negative with increasing temperature confirmed that increasing temperature supported adsorption. On the other hand, it was observed that the entropy changes also contributed to the negative ΔG° value. Regarding standard enthalpy change, the magnitude of ΔH° showed that the adsorption was physisorption (Sun and Wang, 2010). Therefore, it was understood that PH adsorption on GD particles took the form of physisorption. A positive ΔS° value increased the randomness of the solid-solution interface during the adsorption reaction (Yang et al., 2015). The increase in temperature promoted stabilization of the bonds between the binding sites on the PH molecules and GD particles, indicating that the high temperature promoted the adsorption process. Like thermodynamic behaviors, Lütke et al. (2019) also found PH adsorption on activated carbon from black acacia bark.

Table 3
Thermodynamics parameters of phenol and BPB adsorption on GD particles

	Temperature (K)	ΔH° (kJ/mol)	ΔS° (J/mol K)	TΔS° (kJ/mol)	ΔG° (kJ/mol)
Phenol	293	17.96	70.79	20.74	-2.95
	303			21.45	-3.45
	313			22.16	-3.96
	323			22.87	-5.05
BPB	298	31.96	109.22	32.55	-0.98
	308			33.64	-1.30
	318			34.73	-1.75
	323			35.28	-4.33

4. Conclusion

Dye and organic materials are two of the most severe pollutants for water resources due to i) their high production and use and ii) their high potential as pollutants. Both types of pollutants cause rapid changes in water resources' physical and chemical properties. This change adversely affects the health and life of all living things. Therefore, high-efficiency anionic BPB and PH adsorption were aimed to protect water resources in this study.

Within the scope of the study, anionic pollutants were selected. Because adsorption of anionic pollutants remains a severe problem in synthetic supramolecular chemistry. Thus, an essential approach to this problem was presented in this study. Polymeric particles were synthesized quickly with Schiff base chemistry using GA and DETA as monomers for the first time. Appropriate characterization methods proved the successful synthesis of GD particles.

The batch adsorption method was used for bromophenol blue and PH. Optimum conditions for BPB and PH were determined in the experiments carried out with different pH, temperature, initial pollutant concentration, and adsorbent dosage (Table 4). As a result, it was determined that GD polymer particles had a very high capacity of 136.40 mg/g for BPB and 98.26 mg/g for PH. In addition, the mechanism of adsorption was elucidated by adsorption isotherms (Langmuir, Freundlich, Temkin, and D-R), adsorption kinetics (PFO, PSO, W-M intra-particle diffusion, and Elovich), and thermodynamic parameters (Gibb's free energy, enthalpy, and entropy). As a result, it was determined that chemisorption occurred between GD particles and BPB and physical adsorption between GD particles and PH.

In this study, very fast and easy to synthesize, and cheap polymeric particles were synthesized. It was demonstrated that these polymers could be used successfully against BPB and PH, which were important regarding water pollution. The polymeric particles obtained with this synthesis approach are believed to shed important light on future studies.

Table 4
Optimum adsorption conditions for BPB and PH with GD particles

	BPB	PH
pH	4	5
Temperature (ºC)	50	50
Initial concentration (mg/L)	300	10
GD dosage (mg)	10	15
Contact time (min)	180	30

Declarations

Acknowledgements

We want to thank Kastamonu University for its contribution to the conduct of this study.

Author contributions

Conceptualization: Kutalmis Gokkus; Methodology: Cigdem Oter, Kutalmis Gokkus; Formal analysis and investigation: Merilyn Amlani, Cigdem Oter, Kutalmis Gokkus; Writing - original draft preparation: Cigdem Oter, Kutalmis Gokkus, Mahmut Gur; Writing - review and editing: Mahmut Gur, Vural Butun; Supervision: Vural Butun

Data availability Data will be made available upon request.

Competing interests The authors declare no competing interests.

Ethical approval Not applicable

References

1. Abellanas-Perez, P., Carballares, D., Fernandez-Lafuente, R., Rocha-Martin, J.: Glutaraldehyde modification of lipases immobilized on octyl agarose beads: Roles of the support enzyme loading and chemical amination of the enzyme on the final enzyme features. Int. J. Biol. Macromol. **248**, 125853 (2023). https://doi.org/10.1016/j.ijbiomac.2023.125853
2. Ahmed, M.A., Abou-Gamra, Z.M.: Mesoporous MgO nanoparticles as a potential sorbent for removal of fast orange and bromophenol blue dyes. Nanatechnol. Environ. Eng. pp. **1**, 1–11 (2016). https://doi.org/10.1007/s41204-016-0010-7
3. Aliabadi, M., Irani, M., Ismaeili, J., Piri, H., Parnian, M.J.: Electrospun nanofiber membrane of PEO/Chitosan for the adsorption of nickel, cadmium, lead, and copper ions from aqueous solution. Chem. Eng. J. pp. **220**, 237–243 (2013). https://doi.org/10.1016/j.cej.2013.01.021
4. Alorabi, A.Q., Hassan, M.S., Azizi, M.: Fe3O4-CuO-activated carbon composite as an efficient adsorbent for bromophenol blue dye removal from aqueous solutions. Arab. J. Chem. pp. **13**(11), 8080–8091 (2020). https://doi.org/10.1016/j.arabjc.2020.09.039
5. Altaher, H., Khalil, T.E., Abubeah, R.: The effect of dye chemical structure on adsorption on activated carbon: a comparative study. Color. Technol. pp. **130**(3), 205–214 (2014). https://doi.org/10.1111/cote.12086
6. Alves, D.C.S., Coseglio, B.B., Pinto, L.A.A. Jr.: R.S.C. Development of spirulina /chitosan foam adsorbent for phenol adsorption. J. Mol. Liq. pp. **309**, 113256 (2020). https://doi.org/10.1016/j.molliq.2020.113256
7. Andrades, D., Graebin, N.G., Kadowaki, M.K., Ayub, M.A., Fernandez-Lafuente, R., Rodrigues, R.C.: Immobilization and stabilization of different β-glucosidases using the glutaraldehyde chemistry:

Optimal protocol depends on the enzyme. Int. J. Biol. Macromol. pp. **129**, 672–678 (2019). https://doi.org/10.1016/j.ijbiomac.2019.02.057

8. Aygun, A., Karakag, S.Y., Duman, I.: Production of granular activated carbon from fruit stones and nutshells and evaluation of their physical, chemical and adsorption properties. Microporous Mesoporous Mater. pp. **66**, 189–195 (2003). https://doi.org/10.1016/j.micromeso.2003.08.028
9. Bhaumik, M., McCrindle, R., Maity, A.: Efficient removal of Congo red from aqueous solutions by adsorption onto interconnected polypyrrole–polyaniline nanofibres. Chem. Eng. J. pp. **228**, 506–515 (2013). https://doi.org/10.1016/j.cej.2013.05.026
10. Bolto, B., Tran, T., Hoang, M., Xie, Z.: Crosslinked poly (vinyl alcohol) membranes. Prog. Polym. Sci. pp. **34**(9), 969–981 (2009). https://doi.org/10.1016/j.progpolymsci.2009.05.003
11. Chien, S.H., Clayton, W.R.: Application of Elovich equation to the kinetics of phosphate release and sorption in soils. J. Soil. Sci. Soc. Am. J. pp. **44**, 265–268 (1980). https://doi.org/10.2136/sssaj1980.03615995004400020013x
12. Coughlin, R.W., Ezra, F.S.: Role of surface acidity in the adsorption of organic pollutants on the surface of carbon. Environ. Sci. Technol. pp. **2**(4), 291–297 (1968). https://doi.org/10.1021/es60016a002
13. Cremer, P.S., Flood, A.H., Gibb, B.C., Mobley, D.L.: Collaborative routes to clarifying the murky waters of aqueous supramolecular chemistry. Nat. Chem. pp. **10**(1), 8–16 (2018). https://doi.org/10.1038/nchem.2894
14. Demissie, H., An, G., Jiao, R., Ma, G., Liu, L., Sun, H., Wang, D.: Removal of phenolic contaminants from water by in situ coated surfactant on keggin-aluminum nanocluster and biodegradation. Chemosphere. pp. **269**, 128692 (2021). https://doi.org/10.1016/j.chemosphere.2020.128692
15. Djebbar, M., Djafri, F., Bouchekara, M., Djafri, A.: Adsorption of phenol on natural clay. Appl. Water Sci. pp. **2**, 77–86 (2012). https://doi.org/10.1007/s13201-012-0031-8
16. Dubinin, M.M., Radushkevich, L.V.: The equation of the characteristic curve of the activated charcoal, Proceedings of Academy of Sciences, Phys. Chem. Sect. 55, 331–337. (1947)
17. Es'haghi, Z., Vafaeinezhad, F., Hooshmand, S.: Green synthesis of magnetic iron nanoparticles coated by olive oil and verifying its efficiency in extraction of nickel from environmental samples via UV–vis spectrophotometry. Process Saf. Environ. Prot. pp. **102**, 403–409 (2016). https://doi.org/10.1016/j.psep.2016.04.011
18. Feng, C., Ren, P., Huo, M., Dai, Z., Liang, D., Jin, Y., Ren, F.: Facile synthesis of trimethylammonium grafted cellulose foams with high capacity for selective adsorption of anionic dyes from water. Carbohydr. Polym. pp. **241**, 116369 (2020). https://doi.org/10.1016/j.carbpol.2020.116369
19. Freundlich, H.M.F.: Over the adsorption in solution. J. Phys. Chem. pp. **57**, 385–471 (1906)
20. Gale, P.A., Howe, E.N., Wu, X., Spooner, M.J.: Anion receptor chemistry: Highlights from 2016. Coord. Chem. Rev. pp. **375**, 333–372 (2018). https://doi.org/10.1016/j.ccr.2018.02.005
21. Gao, X., Yin, H., Li, M., Xin, L., Zhang, H., Long, H.: Photocatalytic degradation of methyl orange by diethylenetriamine modified chitosan/bentonite composite. Reaction Chem. Eng. pp. (2023).

https://doi.org/10.1039/D3RE00220A

22. Gao, Y., Zheng, H., Wang, J., Wu, J., Li, X., Liu, G.: Physicochemical properties of zein films cross-linked with glutaraldehyde. Polym. Bull. pp. **79**(7), 4647–4665 (2022). https://doi.org/10.1007/s00289-021-03723-9
23. Genta, I., Costantini, M., Asti, A., Conti, B., Montanari, L.: Influence of glutaraldehyde on drug release and mucoadhesive properties of chitosan microspheres. Carbohydr. Polym. pp. **36**(2–3), 81–88 (1998). https://doi.org/10.1016/S0144-8617(98)00022-8
24. Ghaedi, M., Ghaedi, A.M., Negintaji, E., Ansari, A., Vafaei, A., Rajabi, M.: Random forest model for removal of bromophenol blue using activated carbon obtained from Astragalus bisulcatus tree. J. Ind. Eng. Chem. pp. **20**(4), 1793–1803 (2014). https://doi.org/10.1016/j.jiec.2013.08.033
25. Gokkus, K., Sengel, S.B., Yildirim, Y., Hasanbeyoglu, S., Butun, V.: Amine-functionalised poly (glycidyl methacrylate) hydrogels for Congo red adsorption. J. Environ. Eng. Sci. pp. **40**(XXXX), 1–11 (2023). https://doi.org/10.1680/jenes.23.00025
26. Guo, D.D., Li, B., Deng, Z.P., Huo, L.H., Gao, S.: Ladder chain Cd-based polymer as a highly effective adsorbent for removal of Congo red. Ecotoxicol. Environ. Saf. pp. **178**, 221–229 (2019). https://doi.org/10.1016/j.ecoenv.2019.04.042
27. Hasan, N., Lee, J., Kwak, D., Kim, H., Saparbayeva, A., Ahn, H.J., …, Yoo, J.W.: Diethylenetriamine/NONOate-doped alginate hydrogel with sustained nitric oxide release and minimal toxicity to accelerate healing of MRSA-infected wounds. Carbohydr. Polym. pp. **270**, 118387 (2021). https://doi.org/10.1016/j.ecoenv.2019.04.042
28. Ho, Y.S., McKay, G.: Pseudo-second order model for sorption processes. Process. Biochem. pp. **34**(5), 451–465 (1999). https://doi.org/10.1016/S0032-9592(98)00112-5
29. Jiang, H.L., Xu, M.Y., Xie, Z.W., Hai, W., Xie, X.L., He, F.A.: Selective adsorption of anionic dyes from aqueous solution by a novel β-cyclodextrin-based polymer. J. Mol. Struct. pp. **1203**, 127373 (2020). https://doi.org/10.1016/j.molstruc.2019.127373
30. Jiang, X., Ding, W., Li, H., Zhang, Z., Zhong, Z., Liu, H., Zheng, H.: Facile synthesis of Poly (epichlorohydrin-diethylenetriamine) hydrogel for highly selective diclofenac sodium removal. Sep. Purif. Technol. pp. **283**, 120215 (2022). https://doi.org/10.1016/j.seppur.2021.120215
31. Juang, R.S., Wu, F.C., Tseng, R.L.: Mechanism of adsorption of dyes and phenols from water using activated carbons prepared from plum kernels. J. Colloid Interface Sci. pp. **227**(2), 437–444 (2000). https://doi.org/10.1006/jcis.2000.6912
32. Kaşgöz, H., Özgümüş, S., Orbay, M.: Modified polyacrylamide hydrogels and their application in removal of heavy metal ions. Polymer. pp. **44**(6), 1785–1793 (2003). https://doi.org/10.1016/S0032-3861(03)00033-8
33. Khan, M.A., Azad, A.K., Safdar, M., Nawaz, A., Akhlaq, M., Paul, P., …, Abdel-Daim, M.M.: Synthesis and Characterization of Acrylamide/Acrylic Acid Co-Polymers and Glutaraldehyde Crosslinked pH-Sensitive Hydrogels. Gels. pp. **8**(1), 47 (2022). https://doi.org/10.3390/gels8010047

34. Kono, H., Ogasawara, K., Kusumoto, R., Oshima, K., Hashimoto, H., Shimizu, Y.: Cationic cellulose hydrogels cross-linked by poly (ethylene glycol): Preparation, molecular dynamics, and adsorption of anionic dyes. Carbohydr. Polym. pp. **152**, 170–180 (2016). https://doi.org/10.1016/j.carbpol.2016.07.011
35. Kulkarni, V.H., Kulkarni, P.V., Keshavayya, J.: Glutaraldehyde-crosslinked chitosan beads for controlled release of diclofenac sodium. J. Appl. Polym. Sci. pp. **103**(1), 211–217 (2007). https://doi.org/10.1002/app.25161
36. Lagergren, S.: About the theory of so-called adsorption of soluble substances, Kungl Svens Vetensk Akad Handl **24** (1898), 1–39
37. Langmuir, I.: The constitution and fundamental properties of solids and liquids. J. Am. Chem. Soc. pp. **38**, 2221–2295 (1916). https://doi.org/10.4159/harvard.9780674366701.c50
38. Lavrenyuk, H., Kochubei, V., Mykhalichko, O., Mykhalichko, B.: A new flame retardant on the basis of diethylenetriamine copper (II) sulfate complex for combustibility suppressing of epoxy-amine composites. Fire Saf. J. pp. **80**, 30–37 (2016). https://doi.org/10.1016/j.firesaf.2016.01.001
39. Li, K., Wang, J., He, Y., Cui, G., Abdulrazaq, M.A., Yan, Y.: Enhancing enzyme activity and enantioselectivity of Burkholderia cepacia lipase via immobilization on melamine-glutaraldehyde dendrimer modified magnetic nanoparticles. Chem. Eng. J. pp. **351**, 258–268 (2018). https://doi.org/10.1016/j.cej.2018.06.086
40. Liu, J., Yao, S., Wang, L., Zhu, W., Xu, J., Song, H.: Adsorption of bromophenol blue from aqueous samples by novel supported ionic liquids. J. Chem. Technol. Biotechnol. pp. **89**(2), 230–238 (2014). https://doi.org/10.1002/jctb.4106
41. Liu, M., Zheng, J., Wang, L., Hu, Z., Lan, S., Rao, W., …, Yu, C.: Ultrafast and selective adsorption of anionic dyes with amine-functionalized glucose-based adsorbents. J. Mol. Struct. pp. **1263**, 133150 (2022). https://doi.org/10.1016/j.molstruc.2022.133150
42. Lütke, S.F., Igansib, A.V., Pegorarob, L., Dottoa, G.L., Pintob, L.A.A., Cadaval, T.R.S. Jr.: Preparation of activated carbon from black wattle bark waste and its application for phenol adsorption. J. Environ. Chem. Eng. pp. **7**, 103396 (2019). https://doi.org/10.1016/j.jece.2019.103396
43. Martinez, A.W., Caves, J.M., Ravi, S., Li, W., Chaikof, E.L.: Effects of crosslinking on the mechanical properties, drug release and cytocompatibility of protein polymers. Acta Biomater. pp. **10**(1), 26–33 (2014). https://doi.org/10.1016/j.actbio.2013.08.029
44. Mhlongo, J.T., Dlamini, M.L., Nuapia, Y., Etale, A.: Synthesis and application of cationized cellulose for adsorption of anionic dyes. Materials Today: Proceedings, 62, S133-S140. (2022). https://doi.org/10.1016/j.matpr.2022.02.100
45. Migneault, I., Dartiguenave, C., Bertrand, M.J., Waldron, K.C.: Glutaraldehyde: behavior in aqueous solution, reaction with proteins, and application to enzyme crosslinking. Biotechniques. pp. **37**(5), 790–802 (2004). https://doi.org/10.2144/04375RV01
46. Mohanty, K., Das, D., Biswas, M.N.: Adsorption of phenol from aqueous solutions using activated carbons prepared from Tectona grandis sawdust by ZnCl2 activation. Chem. Eng. J. pp. **115**, 121–

131 (2005). https://doi.org/10.1016/j.cej.2005.09.016

47. Mohd, N.H., Kargazadeh, H., Miyamoto, M., Uemiya, S., Sharer, N., Baharum, A., …, Othaman, R.: Aminosilanes grafted nanocrystalline cellulose from oil palm empty fruit bunch aerogel for carbon dioxide capture. J. Mater. Res. Technol. pp. **13**, 2287–2296 (2021). https://doi.org/10.1016/j.jmrt.2021.06.018
48. More, S.M., Kulkarni, R.V., Sa, B., Kayane, N.V.: Glutaraldehyde-crosslinked poly (vinyl alcohol) hydrogel discs for the controlled release of antidiabetic drug. J. Appl. Polym. Sci. pp. **116**(3), 1732–1738 (2010). https://doi.org/10.1002/app.31627
49. Nayunigari, M.K., Das, R., Maity, A., Agarwal, S., Gupta, V.K.: Folic acid modified cross-linked cationic polymer: Synthesis, characterization, and application of the removal of Congo red dye from aqueous medium. J. Mol. Liq. pp. **227**, 87–97 (2017). https://doi.org/10.1016/j.molliq.2016.11.129
50. Nirmala, G., Murugesan, T., Rambabu, K., Sathiyanarayanan, K., Show, P.L.: Adsorptive removal of phenol using banyan root activated carbon. Chem. Eng. Commun. pp. **208**(6), 831–842 (2021). https://doi.org/10.1080/00986445.2019.1674839
51. Ong, W.S., Smaldone, R.A., Dodani, S.C.: A neutral porous organic polymer host for recognizing anionic dyes in water. Chem. Sci. pp. **11**(29), 7716–7721 (2020). 10.1039/d0sc02941f
52. Pardo, L., Cecilia, J.A., López-Moreno, C., Hernández, V., Pozo, M., Bentabol, M.J., Franco, F.: Influence of the structure and experimental surfaces modifications of 2: 1 clay minerals on the adsorption properties of methylene blue. Minerals. pp. **8**(8), 359 (2018). https://doi.org/10.3390/min8080359
53. Ramires, P.A., Milella, E.: Biocompatibility of poly (vinyl alcohol)-hyaluronic acid and poly (vinyl alcohol)-gellan membranes crosslinked by glutaraldehyde vapors. J. Mater. Science: Mater. Med. pp. **13**, 119–123 (2002). https://doi.org/10.1023/A:1013667426066
54. Repo, E., Warchoł, J.K., Bhatnagar, A., Sillanpää, M.: Heavy metals adsorption by novel EDTA-modified chitosan–silica hybrid materials. J. Colloid Interface Sci. pp. **358**(1), 261–267 (2011). https://doi.org/10.1016/j.jcis.2011.02.059
55. Şenkal, B.F., Biçak, N.: Glycidyl methacrylate based polymer resins with diethylene triamine tetra acetic acid functions for efficient removal of Ca (II) and Mg (II). Reactive and Functional Polymers. pp. **49**(2), 151–157 (2001). https://doi.org/10.1016/S1381-5148(01)00075-X
56. Shahbazi, A., Younesi, H., Badiei, A.: Functionalized SBA-15 mesoporous silica by melamine-based dendrimer amines for adsorptive characteristics of Pb (II), Cu (II) and Cd (II) heavy metal ions in batch and fixed bed column. Chem. Eng. J. pp. **168**(2), 505–518 (2011). https://doi.org/10.1016/j.cej.2010.11.053
57. Song, W., Gao, B., Xu, X., Xing, L., Han, S., Duan, P., …, Jia, R.: Adsorption–desorption behavior of magnetic amine/Fe3O4 functionalized biopolymer resin towards anionic dyes from wastewater. Bioresour. Technol. pp. **210**, 123–130 (2016). https://doi.org/10.1016/j.biortech.2016.01.078
58. Sridar, R., Ramanane, U.U., Rajasimman, M.: ZnO nanoparticles-Synthesis, characterization and its application for phenol removal from synthetic and pharmaceutical industry wastewater. Environ. Nanotechnol Monit. Manag. pp. **10**, 388–393 (2018). https://doi.org/10.1016/j.enmm.2018.09.003

59. Sullivan, M.R., Yao, W., Tang, D., Ashbaugh, H.S., Gibb, B.C.: The thermodynamics of anion complexation to nonpolar pockets. J. Phys. Chem. B. pp. **122**(5), 1702–1713 (2018). https://doi.org/10.1021/acs.jpcb.7b12259
60. Sun, C.L., Wang, C.S.: Estimation on the intramolecular hydrogen-bonding energies in proteins and peptides by the analytic potential energy function. J. Mol. Struct. Theochem. pp. **956**, 38–43 (2010). https://doi.org/10.1016/j.theochem.2010.06.020
61. Temkin, M.I., Pyzhev, V.: Kinetics of ammonia synthesis on promoted iron catalyst. Acta Phys. Chim. USSR. pp. **12**, 327–356 (1940)
62. Tümsek, F., Demir, S.: Kil-Karbon Kompozitlerin Azot ve Fenol Adsorpsiyon Kapasitelerinin Belirlenmesi. J. ESOGU Eng. Arc Fac. pp. **27**, 100–109 (2019). https://doi.org/10.31796/ogummf.551702
63. Wang, H., Paul, D.R., Chung, T.S.: Surface modification of polyimide membranes by diethylenetriamine (DETA) vapor for H2 purification and moisture effect on gas permeation. J. Membr. Sci. pp. **430**, 223–233 (2013). https://doi.org/10.1016/j.memsci.2012.12.008
64. Weber, W.J., Morris, J.C.: Kinetics of adsorption on carbon from solution. J. Sanit. Eng. Div. pp. **89**, 31–60 (1963). https://doi.org/10.1061/JSEDAI.0000430
65. Xiang, Y., Gao, M., Shen, T., Cao, G., Zhao, B., Guo, S.: Comparative study of three novel organo-clays modified with imidazolium-based gemini surfactant on adsorption for bromophenol blue. J. Mol. Liq. pp. 286 (2019). https://doi.org/10.1016/j.molliq.2019.110928
66. Xu, M.Y., Jiang, H.L., Xie, Z.W., Li, Z.T., Xu, D., He, F.A.: Highly efficient selective adsorption of anionic dyes by modified β-cyclodextrin polymers. J. Taiwan Inst. Chem. Eng. pp. **108**, 114–128 (2020). https://doi.org/10.1016/j.jtice.2020.01.005
67. Yagub, M.T., Sen, T.K., Afroze, S., Ang, H.M.: Dye and its removal from aqueous solution by adsorption: a review. Adv. Colloid Interface Sci. pp. **209**, 172–184 (2014). https://doi.org/10.1016/j.cis.2014.04.002
68. Yang, G., Tang, L., Zeng, G., Cai, Y., Tang, J., Pang, Y., Zhou, Y., Liu, Y., Wang, J., Zhang, S., Xiong, W.: Simultaneous removal of lead and phenol contamination from water by nitrogen-functionalized magnetic ordered mesoporous carbon. Chem. Eng. J. pp. **259**, 854–864 (2015). https://doi.org/10.1016/j.cej.2014.08.081
69. Yang, Y., Chuah, C.Y., Bae, T.H.: Highly efficient carbon dioxide capture in diethylenetriamine-appended porous organic polymers: Investigation of structural variations of chloromethyl monomers. J. Ind. Eng. Chem. pp. **88**, 207–214 (2020). https://doi.org/10.1016/j.jiec.2020.04.014
70. You, L., Huang, C., Lu, F., Wang, A., Liu, X., Zhang, Q.: Facile synthesis of high performance porous magnetic chitosan-polyethylenimine polymer composite for Congo red removal. Int. J. Biol. Macromol. pp. **107**, 1620–1628 (2018). https://doi.org/10.1016/j.ijbiomac.2017.10.025
71. You, L., Wu, Z., Kim, T., Lee, K.: Kinetics and thermodynamics of Bromophenol blue adsorption by a mesoporous hybrid gel derived from tetraethoxysilane and bis (trimethoxysilyl) hexane. J. Colloid Interface Sci. pp. **300**(2), 526–535 (2006). https://doi.org/10.1016/j.jcis.2006.04.039

72. Zelenka, T., Simanova, K., Saini, R., Zelenkova, G., Nehra, S.P., Sharma, A., Almasi, M.: Carbon dioxide and hydrogen adsorption study on surface-modified HKUST-1 with diamine/triamine. Sci. Rep. pp. **12**(1), 17366 (2022). https://doi.org/10.1038/s41598-022-22273-2
73. Zhang, Y., Qu, R., Sun, C., Wang, C., Ji, C., Chen, H., Yin, P.: Chemical modification of silica-gel with diethylenetriamine via an end-group protection approach for adsorption to Hg (II). Appl. Surf. Sci. pp. **255**(11), 5818–5826 (2009). https://doi.org/10.1016/j.apsusc.2009.01.011

Figures

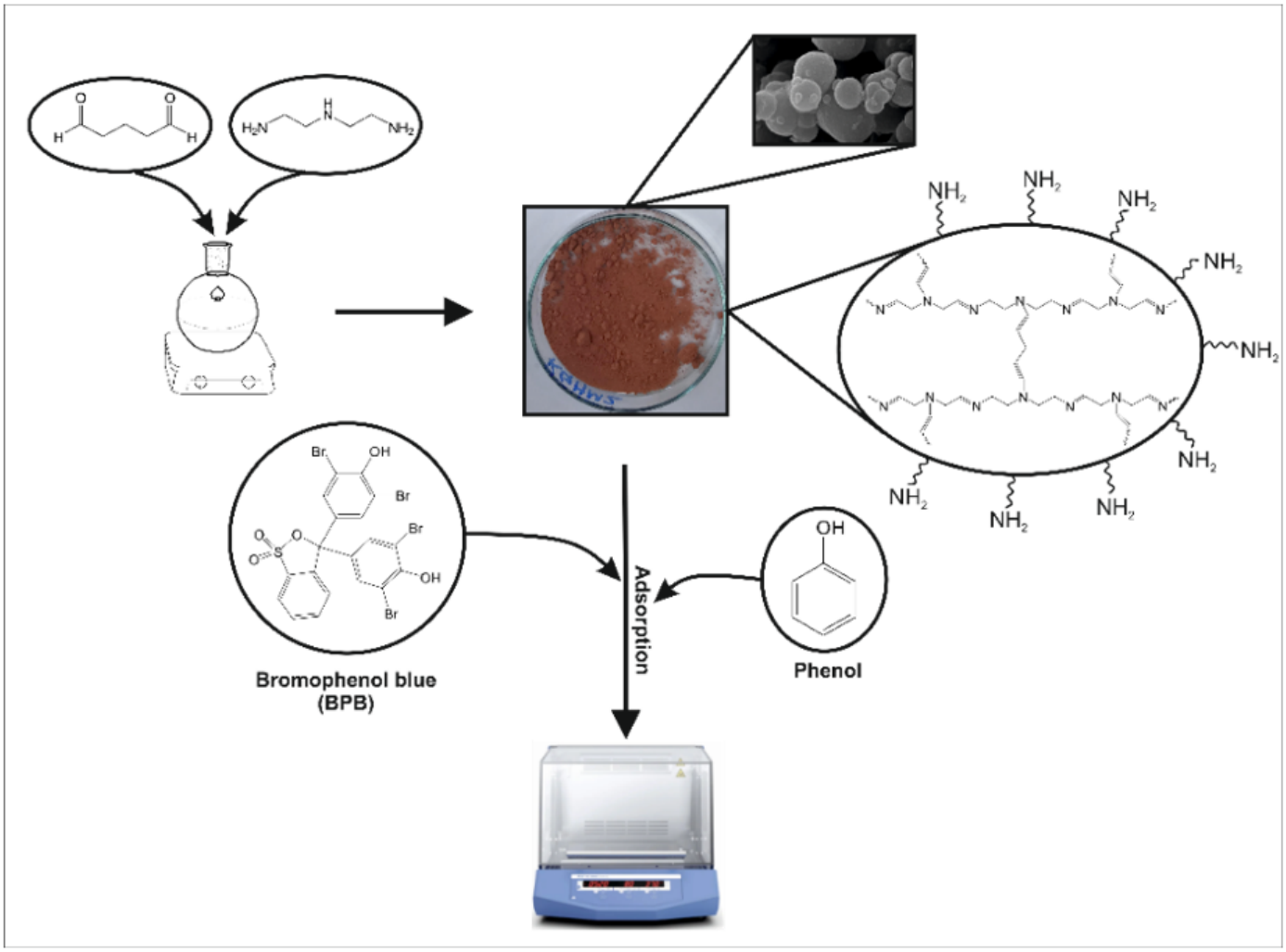

Figure 1

Schematic summary of the study

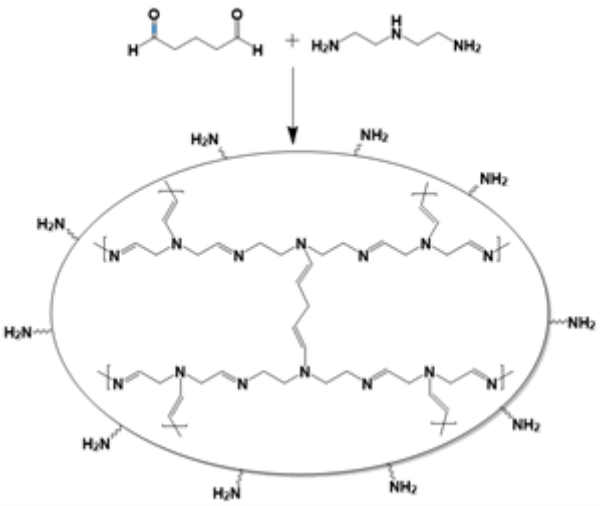

Figure 2

Synthesis of GD polymer particles

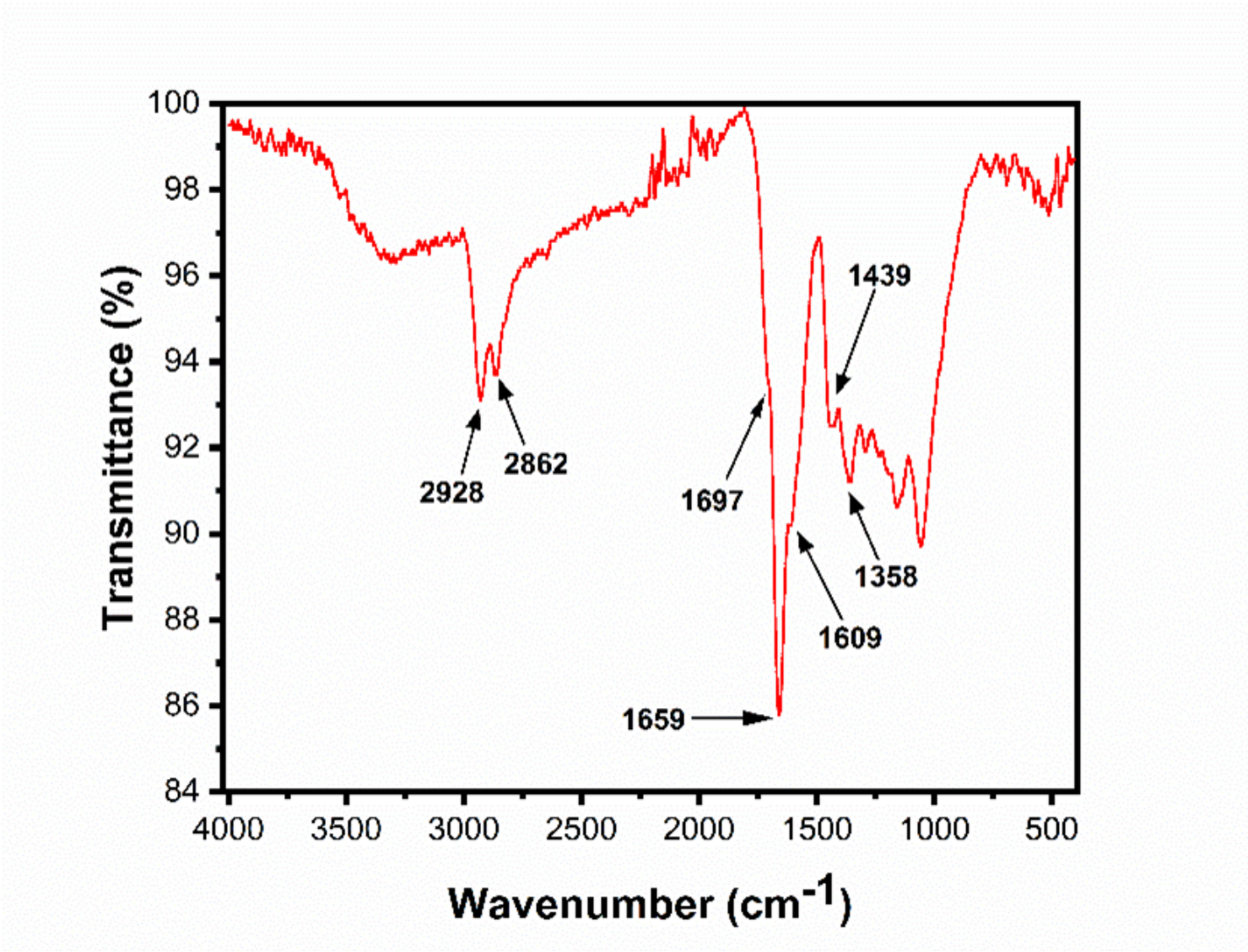

Figure 3

FT-IR spectrum of GD polymer particles

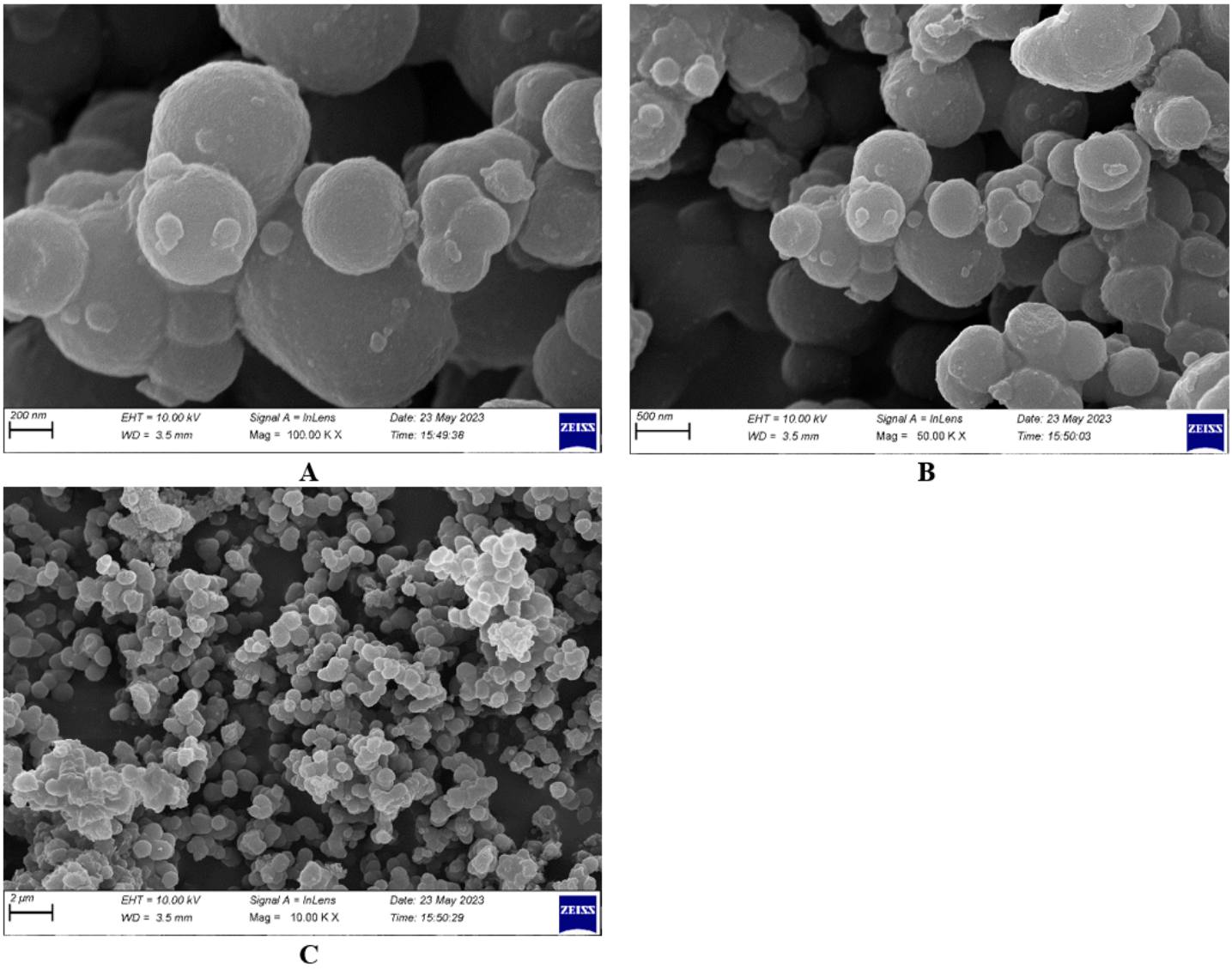

Figure 4

SEM micrographs of GD polymer particles

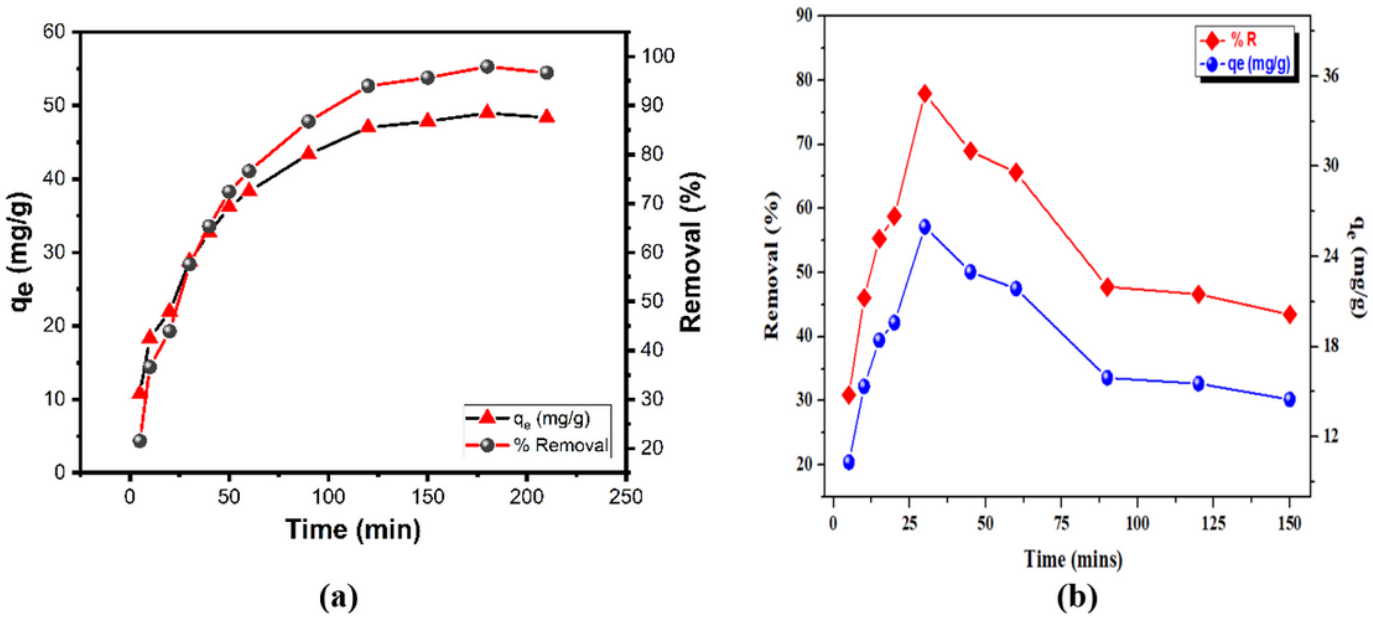

Figure 5

Effects of contact time on (a) BPB (initial conc.: 100 mg/L; T: 25ºC; adsorbent: 50 mg; V: 25 mL) and (b) phenol adsorption (pH:5.5; initial conc. 50 mg/L; adsorbent 15 mg, V:10 mL, T:25°C, 400 rpm)

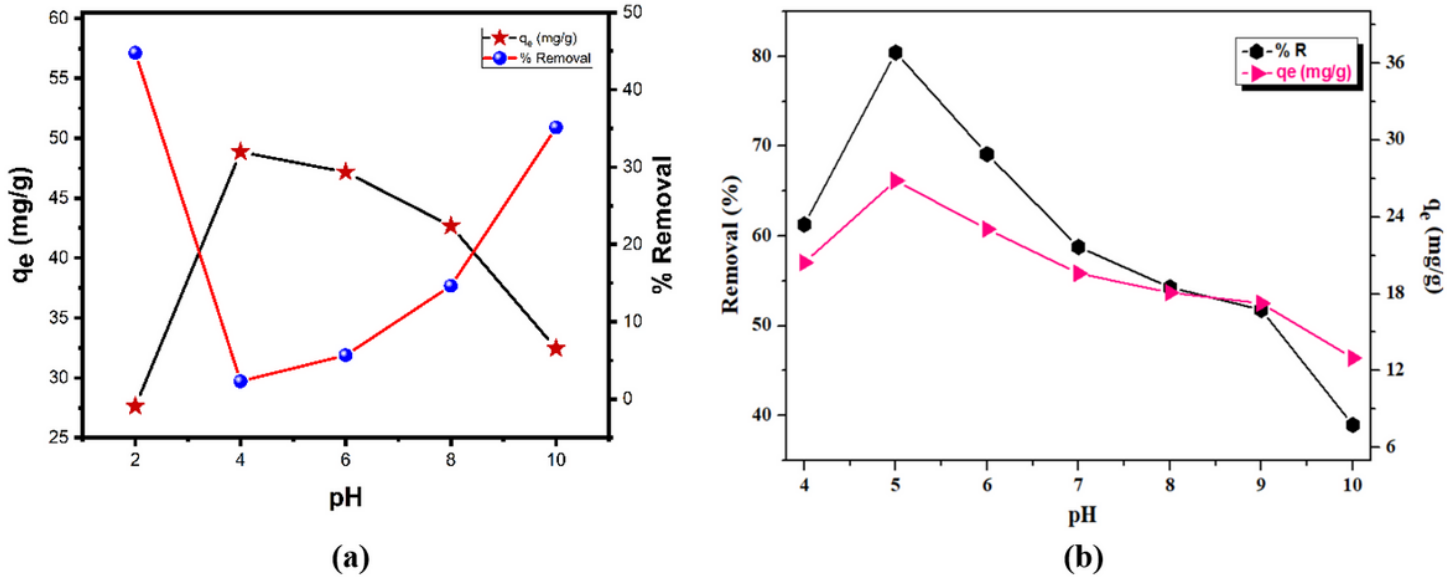

Figure 6

Effects of pH on (a) BPB (t: 180 min; concentration: 100 mg/L; T: 25ºC; adsorbent: 50 mg; V: 25 mL) and (b) phenol adsorption (t: 30 min; initial conc. 50 mg/L; adsorbent 15 mg, V:10 mL, T:25°C, 400 rpm)

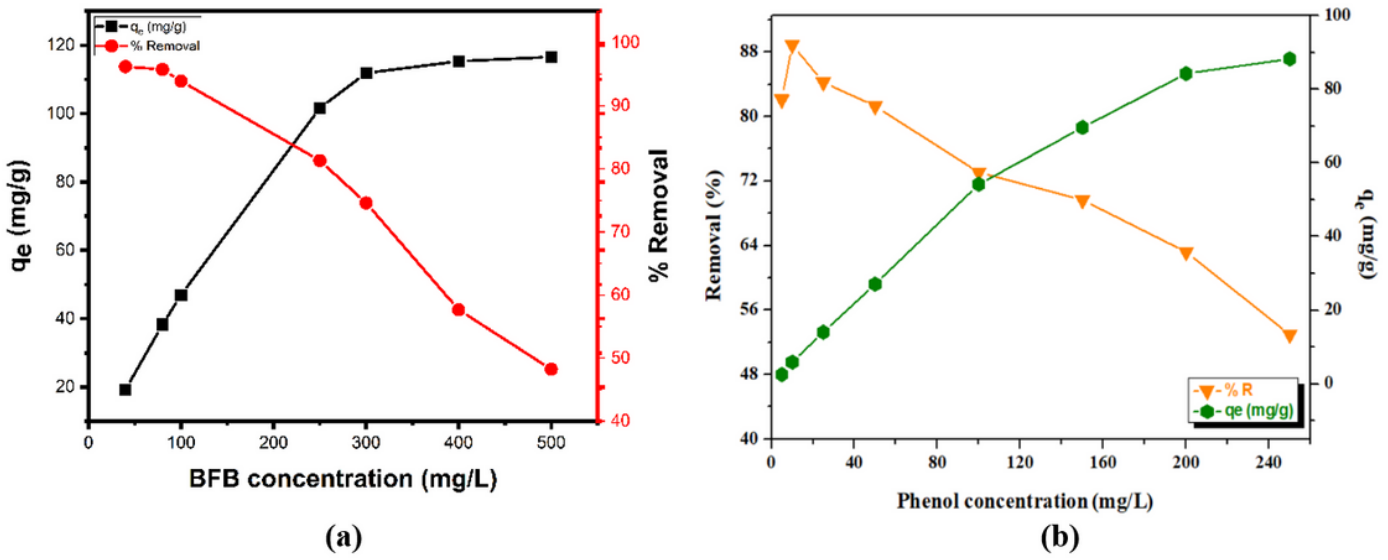

Figure 7

Effects of initial concentration on (a) BPB (t: 180 min; pH: 4.0; T: 25°C; adsorbent: 50 mg; V: 25 mL) and (b) phenol adsorption (t: 30 min; pH: 5.0; adsorbent 15 mg, V:10 mL, 400 rpm)

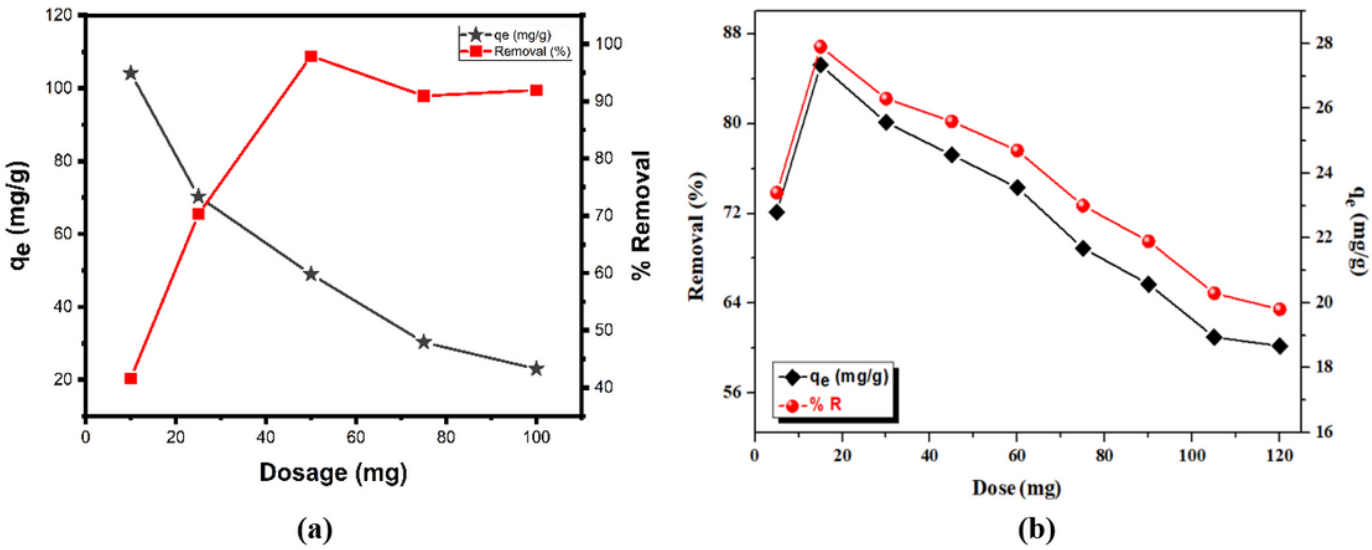

Figure 8

Effects of adsorbent dosage on (a) BPB (t: 180 min; concentration: 100 mg/L; pH: 4.0; T: 25°C; adsorbent: 50 mg; V: 25 mL) and (b) phenol adsorption (t: 30 min; pH: 5.0; adsorbent 15 mg, V:10 mL, 400 rpm)

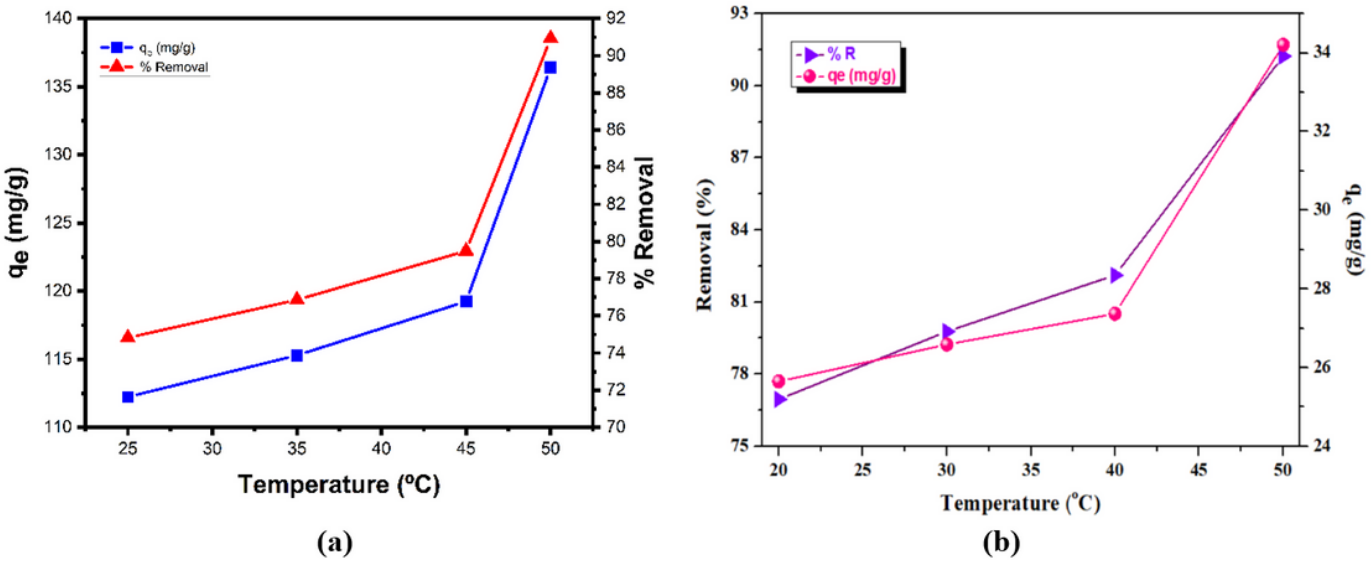

Figure 9

Effects of temperature on (a) BPB (t: 180 min; concentration: 100 mg/L; pH: 4.0; adsorbent: 50 mg; V: 25 mL) and (b) phenol adsorption (t: 30 min; pH: 5.0; initial conc. 50 mg/L; adsorbent 15 mg, V:10 mL, 400 rpm)

Supplementary Files

This is a list of supplementary files associated with this preprint. Click to download.

- GDparticlesSupplementaryDocument23.10.2023.pdf